Chapter 9

Direct Antiproton Observations: Electronic Damping

Direct observations of the cyclotron motion of the antiprotons are made by using a resonant preamplifier at $\nu_c'(\overline{p})$ connected across two of the segments of the quad ring [97]. This scheme, also provides direct resistive cooling of the antiproton cyclotron motion, and alleviates the need to rely on the electrons for damping.

In this chapter we present the use of direct cyclotron detection, the obtainable resolution, and describe use of this technique in performing systematic studies regarding trap polarity in order to compare protons and antiprotons. We also discuss more refined measurements of the axial frequency of antiprotons including coherent detection and the locking of the axial frequency to an external oscillator analogous to the electron system (Chapter 6). The techniques described in this chapter apply equally well to the detection and measurement of protons.

9.1 Direct Cyclotron Detection

Direct detection of the cyclotron oscillation is analogous to the axial detection except, unlike the axial motion which depends only on the electrostatic quadrupole field, the cyclotron motion also depends on the state of the magnetic field. A resonant circuit tuned to about 89 MHz is connected to the ring electrode as shown in Fig. 5.5. At 5.9 T, the modified cyclotron frequency is nearly centered in the detector resonant bandwidth. At 4 K, a signal at $\nu_c'(\overline{p})$ is not observable,

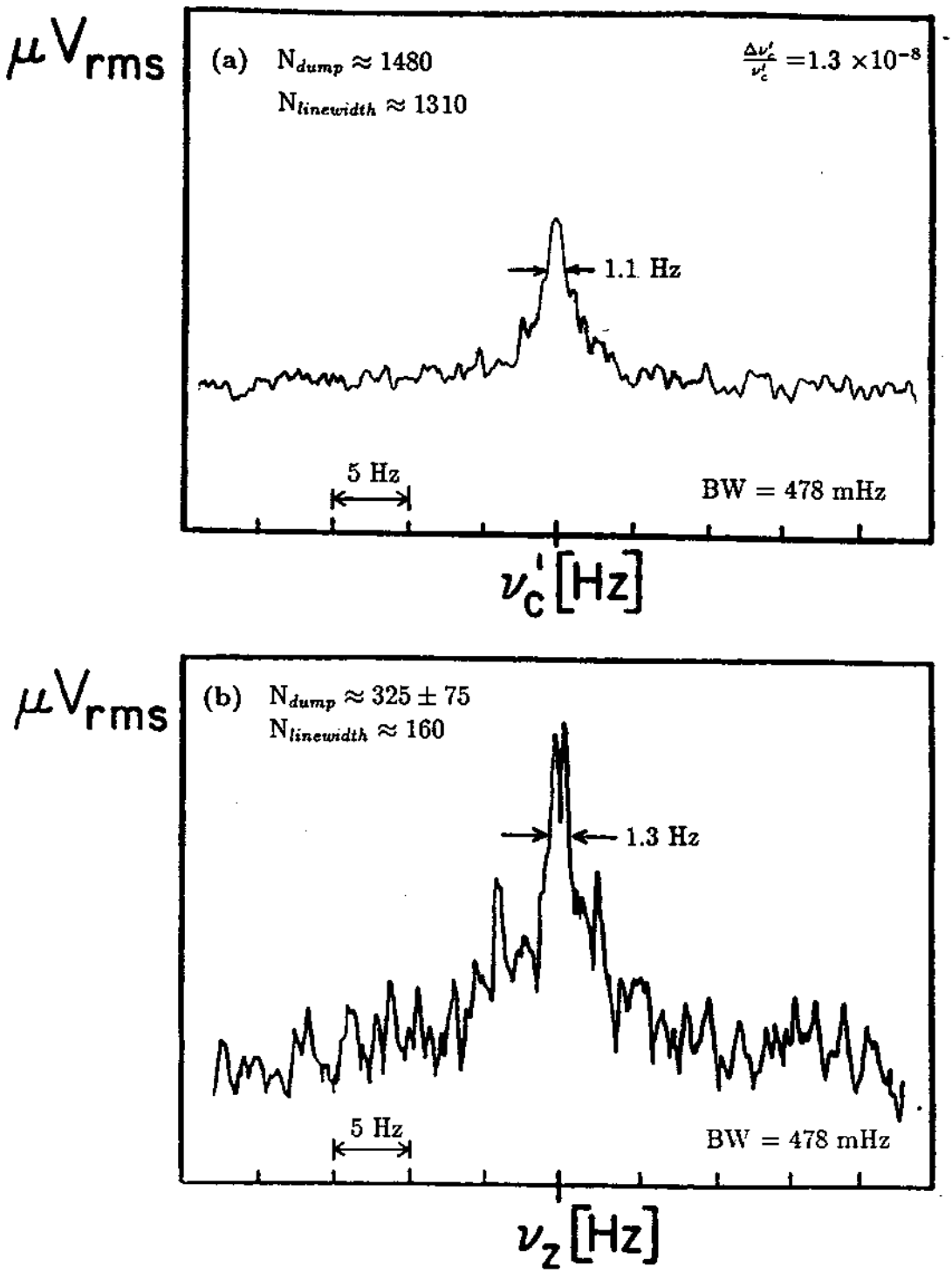

Figure 9.1: Direct observations of the antiproton oscillation frequencies on an HP 3561A signal analyzer after being mixed down to approximately 50 kHz. (a) The antiproton modified cyclotron frequency. (b) The antiproton axial frequency.

but for sufficient heat ν_c' ($\overline{p}$) can be directly observed as shown in Fig. 9.1(a). Without electrons in the trap, the antiproton damping time τ is on the order of hundreds of seconds, thus for sufficiently high temperatures, one can directly observe the residual heat of the particles by observing the frequency spectrum at 89 MHz. Unlike the bolometric technique described in Chapter 8 no external resonant drives are applied to the system during aquisition of the signal. With this technique we are sensitive to as few as 40 antiprotons (or protons) though systematic shifts are observed for the levels of resonant ν_c' heating required to observe so few with our present detection sensitivity (Chapter 5).

A system of more than 200 antiprotons is easily observed with only slight heating applied by driving on the magnetron sideband frequency $\nu_c' + \nu_m$. This frequency, applied either to the balanced drive on the ring or on both endcaps, serves to cool (i.e. reduce) the magnetron orbit, centering the antiprotons in the trap with a lower cooling limit than is possible with the drive at $\nu_z + \nu_m$ [13].

For large amounts of heating, the lineshape grows asymmetrically to lower frequencies (Chapter 10, Fig. 10.13). In general, a corresponding broadening as a function of cyclotron heating is not observed in the axial signal.

9.1.1 Simultaneous Measurements of ν_c' and ν_z

Along with the ability to directly detect cyclotron signals with reduced amounts of heat, small and narrow axial signals can be observed as shown in Fig. 9.1. For purposes of the mass comparison, the cyclotron ν_c' and axial ν_z signal can now be simultaneously but *independently* measured. Both measurements are then used to compute the correction frequency $\nu_z^2/2\nu_c'$ to obtain the free space cyclotron frequency by the now familiar relationship

$$\nu_c = \nu_c' + \frac{\nu_z^2}{2\nu_c'}. \tag{9.1}$$

The simultaneous observation of ν_c' and ν_z at a fixed voltage is the method we have used most extensively for determinations of the antiproton (and proton) free space cyclotron frequencies reported in this thesis. Unlike the ν_c' versus voltage method, this method is independent of absolute trap voltage, since the sum of

ν_c' and $\nu_z^2/2\nu_c'$ is independent of voltage. Figure 9.1 shows the high resolution that can be obtained by direct observation of ν_c' and ν_z. Both detected spectra shown were observed using an HP3561A Signal Analyzer after the signals were mixed down to about 50 kHz (see Fig. 5.4). No external drives are applied during the detection of these signals. The signals are just observations of the residual heat in the respective orthogonal oscillations of the confined antiprotons.

If allowed to resistively damp to 4 K, the signals disappear into the noise floor but a dip, as in the case of electrons, is not observed. To get sufficient signal to noise we must add small quantities of heat. To give a perspective of the much smaller amounts of heat we apply, we can usually heat the motion enough to observe the cyclotron frequency for many minutes with a -35 dBm drive applied on the sideband $\nu_c' + \nu_m$ for 5 seconds. With the bolometric technique described in chapter 8, we continuously apply about -20 dBm on ν_c' .

For small clouds (< 2000) and with only little heating, the axial and cyclotron motions seem completely uncoupled if the trap compensation is adjusted properly. Heat can be applied to either degree of freedom by direct drives or using the appropriate magnetron sideband drives.

The ability to easily study the heat exchange between the two modes is very useful. For small clouds, we can turn on the coupling by mistuning the trap anharmonicity (analogous to the electron case in Chapter 6) or by driving the particles to extremely large amplitudes. If sufficient cooling electrons remain in the trap, the coupling seems aided by collision mechanisms. For large clouds, collisional mechanisms appear to keep the normal modes nearly in thermal equilibrium with each other.

With present sensitivities, the best resolution obtained with this method of observing residual heat in the normal modes is $\Delta\nu_c' \approx 1$ Hz (10^{-8}), and $\Delta\nu_z \approx$ 400 mHz (2×10^{-7}). The limiting cyclotron linewidth appears to be an indication of the trapped number, although field stability, or broadening by the sampling of field gradients or trap anharmonicity may result from the slight heating of the antiprotons.

9.1.2 Cyclotron Measurements vs. Voltage

Directly observing cyclotron frequencies by the method outlined in the previous section has some very important advantages. With just this one amplifier it is possible to determine the free space cyclotron frequency by measuring ν_c' as a function of trapping voltage. The extrapolation to zero trap voltage (where V=0 is when $\nu_z = 0$) gives a measurement of the free space cyclotron frequency, since the perturbation of the quadrupole potential no longer exists. In Fig. 9.2(a), measurements of ν_c' are plotted as a function of voltage. In Fig. 9.2(b), the residuals of the measured points from the least squares fit are shown which in this case are distributed in a near random fashion.

The analysis of these measurements is an extremely valuable check on electrostatic systematics. The functional form of $\nu_c'(V_0)$ for a perfect trap deviates slightly from a line at high trapping potentials. From (2.12) the cyclotron frequency ν_c' is

$$\nu_c' = \nu_c - \frac{\nu_z^2}{2\nu_c'} + F(\epsilon, \theta). \tag{9.2}$$

The term $F(\epsilon,\theta)/\nu_c'$ is 3.6×10^{-11} with our present operating parameters. Neglecting this term, we can expand in terms of the small parameter (ν_z/ν_c') giving

$$\nu_c' = \nu_c - \frac{\alpha V_0}{2\nu_c} - \frac{\alpha^2 V_0^2}{4\nu_c^2 \nu_c'} - ..... \tag{9.3}$$

where $\alpha \equiv (C_2 e/md^2)$. For low voltages (where most perturbations have the largest influence), the second order term is small and the linear form is sufficient.

Because antiprotons and protons are essentially identical, but of opposite charge, this technique can be used to perform and understand systematic studies with regard to electrostatic perturbations and trapping polarity. The importance of understanding systematics related with comparing particles of opposite polarity in Penning traps is well known [97] but has proven troublesome as evident in early attempts to compare the mass of the proton and the electron [99,100]. These earlier measurements were limited in the uncertainty of the relative positions of opposite polarity particles in the trap.

For the antiproton-proton mass comparison, we have performed several determinations of $\nu_c'(\overline{p})$ as a function of voltage and studied the slope, intercept, and

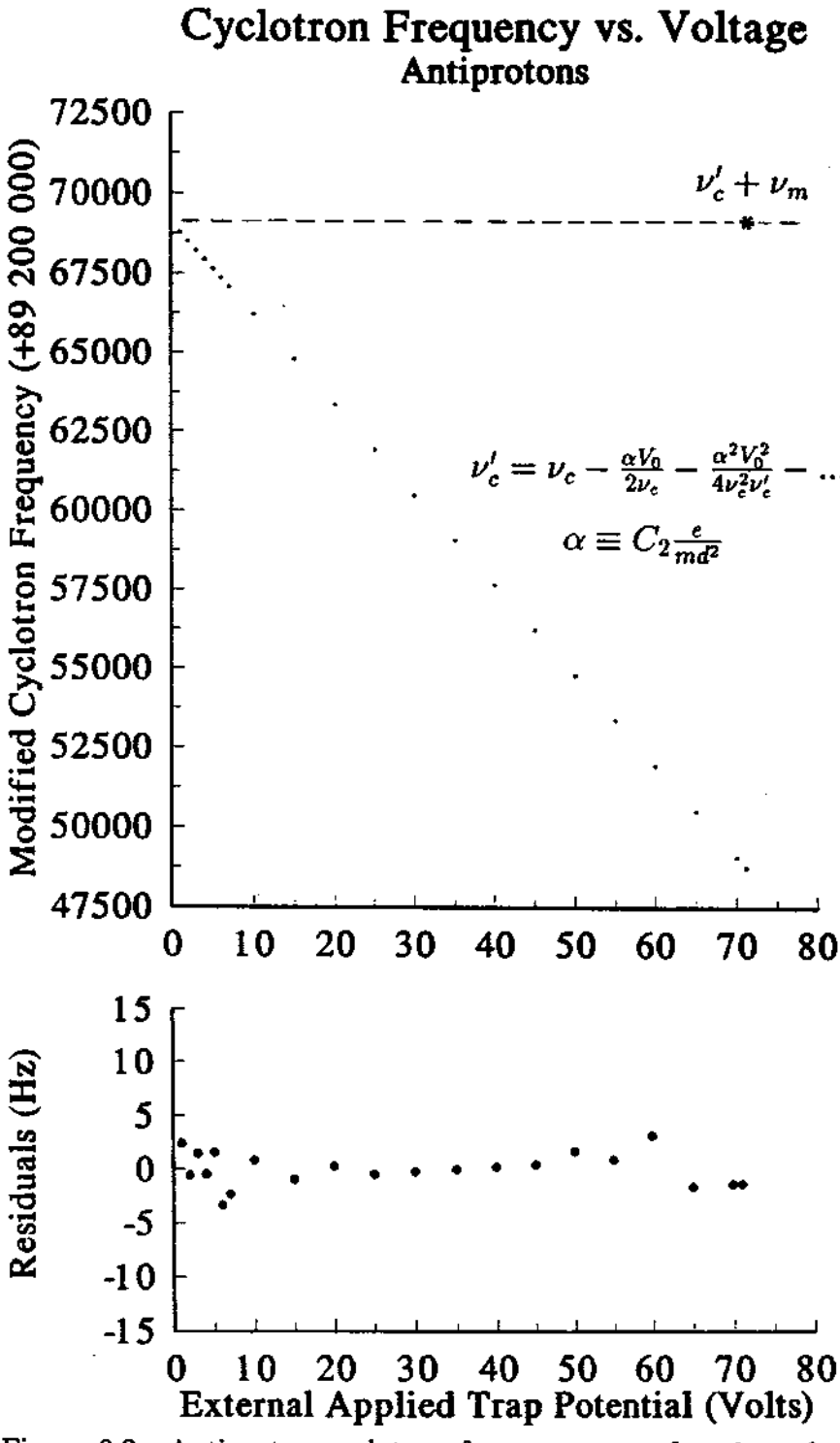

Figure 9.2: Antiproton cyclotron frequency as a function of trap voltage and the residuals of the linear fit. Analogous measurements, but with opposite trap polarity, are performed using protons.

scatter of such measurements. The extrapolated intercepts are direct measurements of the free space cyclotron frequency which can be compared to measurements made at a fixed voltage. For the extrapolation to be accurate, the absolute zero voltage point on the trap must be known. In fact, offsets in the trap voltage (evidently from contact potentials) are clearly observed with this technique when we reverse the trap polarity. In Chapter 10, we present comparison data using protons and antiprotons. We also compare these observations with observations of the axial frequency taken at a fixed trapping potential, but with opposite polarity.

9.2 Phase Sensitive Detection

9.2.1 Axial Motion

Cleaning Residual Electrons

The direct and simultaneously detected 'heat' signals are easily observable even though there may remain small numbers of electrons from the initial reduction procedure outlined in Chapter 4. For high precision measurements it becomes necessary to eliminate the possible perturbations arising from impurity ions. We have been able to obtain antiprotons clouds of up to 2000 antiprotons which have several signs of being free of electrons. The clean clouds are obtained with repeated applications of the drive and dip procedure to yet lower voltages, typically 300 mV and then 100 mV. Often in these last two steps, we observe antiprotons leaking from the trap. The effectiveness on expelling the last few electrons seems correlated with the use of the axial magnetron sideband drive to keep the electrons centered and on resonance during the drive and dip procedure.

We observe the effectiveness of our technique in three different ways. First, we look for axial heating of the few remaining electrons by severe cyclotron heating of the antiprotons as described in chapter 8. Second, we can measure the damping constants of the axial and cyclotron motions of the antiprotons and observe that they increase as a function of dipping and converge to the expected resistive damping rates which are much slower than when electrons are present. A third indicator is when we can obtain coherent axial antiproton responses to an external

drive analogous to the observations with electrons in Chapter 6. We also cannot obtain coherent axial resonances of electrons when antiprotons are simultaneously present in the trap. Similarly, coherent proton resonances can only be achieved when few ($N_{ions} << N_{protons}$) or no other positive ions are identified to be present in the trap. The proton observations are consistent with the experience of others [106].

Coherent Axial Response

The success of preferentially removing electrons from the trap has allowed us to use phase sensitive detection on the axial motion of the antiprotons. The scheme is entirely analogous to the case for electrons except that the signal is much weaker for the more massive, slow moving antiprotons (since the resistive damping of the axial motion is proportional to 1/m). The typical trap voltage is +71.6 Volts producing an antiproton axial frequency of about 1.91 MHz. The ring is modulated at $\nu_{mod} = 63.07$ kHz, or ν_{mod}/ν_z=0.032 (for electrons ν_{mod}/ν_z=0.022 was used).

An example of a coherent axial response of antiprotons is shown in Fig. 9.3. The response signal is obtained from a Stanford Research Systems SR510 Lock-in Amplifier when the axial and ring modulation drive strengths are finely adjusted. As with the electrons, the ability to achieve good signal to noise is dependent upon simultaneous application of axial magnetron sideband cooling near $\nu_z + \nu_m$, but not directly on it. When drive strengths and trap harmonicity are optimally tuned, coherent signals can be detected even as the directly observed 'heat' signals of $\nu_z(\overline{p})$ and $\nu_c'(\overline{p})$ damp away. The ability to observe the antiprotons with much less heat should result in less perturbed measurements on smaller numbers.

Locked Axial Frequency

Once we obtain the dispersion curve as shown in Fig. 9.3, we can lock the axial frequency to an external oscillator analogous to the technique for electrons. Figure 9.4(a) shows the locked axial response of antiprotons at $\nu_z(\overline{p})$ analogous to the locked electron response shown in Fig. 6.2. This observed trace is highly

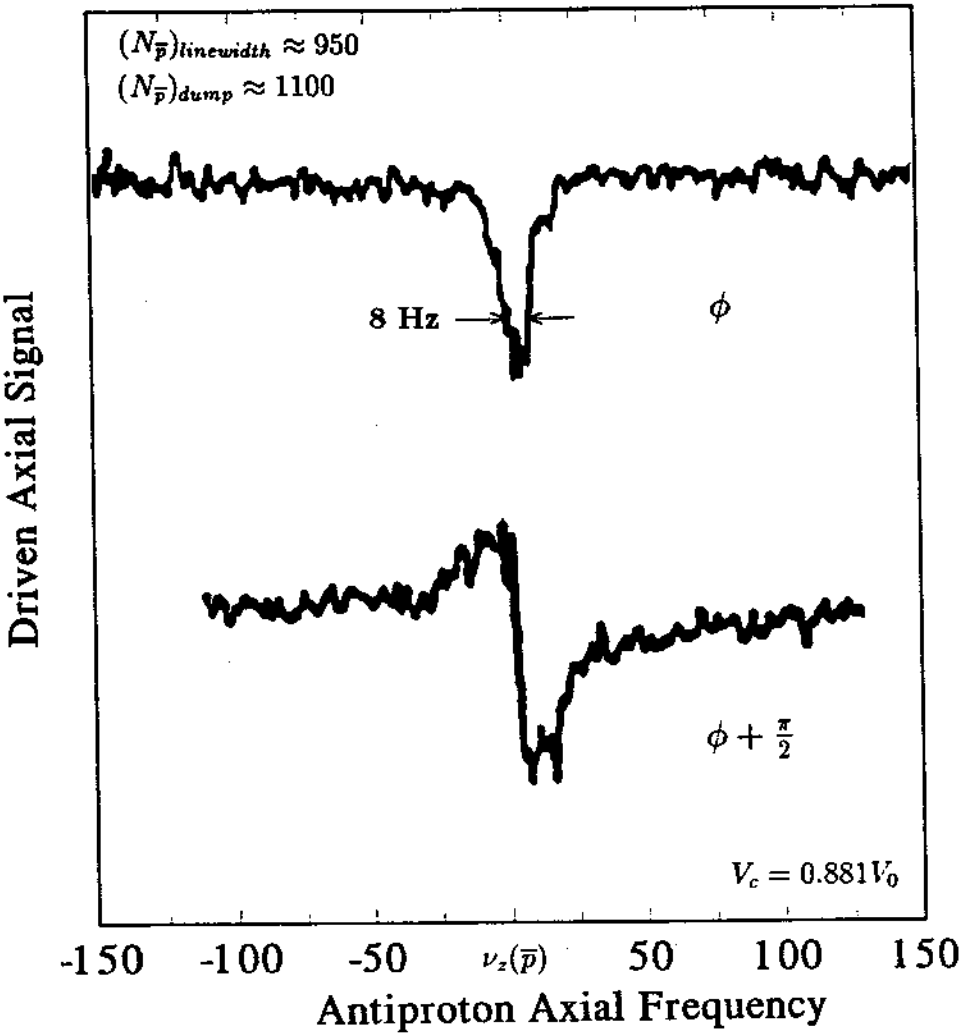

Figure 9.3: Phase sensitive detected axial signal of weakly driven antiprotons.

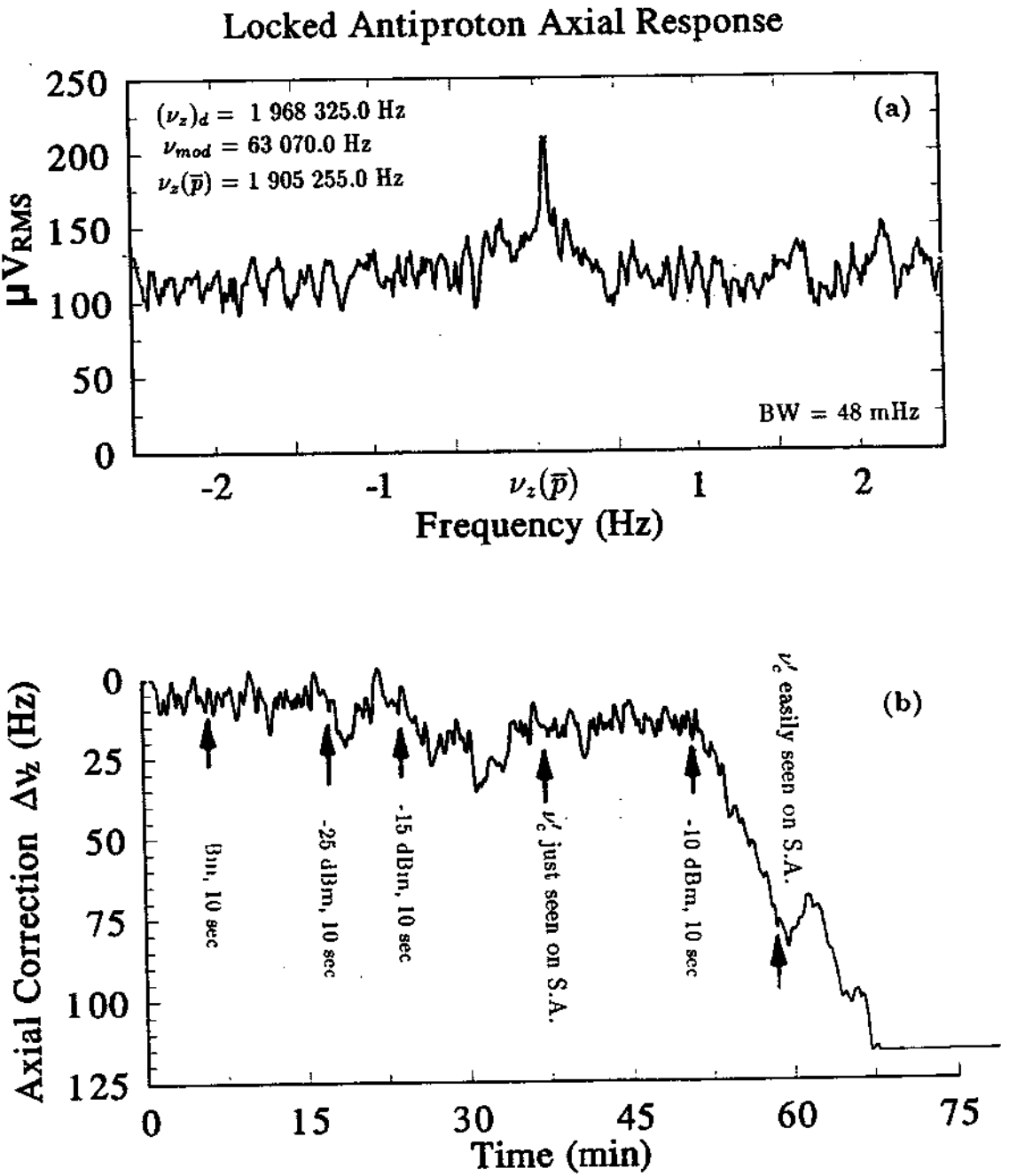

Figure 9.4: (a) Highly averaged locked antiproton axial response to drives at $(\nu_z + \nu_{mod})_d$ with the ring potential modulated at ν_{mod}. (b) Trap voltage feedback signal correcting for heating introduced with a weak cyclotron sideband drive at $\nu_c' + \nu_m$.

averaged using an HP3561A Signal Analyzer with a bandwidth of 48 mHz which limits the observed linewidth.

Figure 9.4(b) shows the voltage feedback signal to keep the axial motion of about 380 antiprotons locked. The lock, which is accomplished with a feedback integration time of about 20 seconds, can be held for hours. In Fig. 9.4(b) the lock is severly perturbed by applying successively stronger excitation drive signals at $\nu_c' + \nu_m$ while attempting to simultaneously observe direct cyclotron heating as described in Section 9.1. Eventually, the signal is kicked out of lock, though a direct cyclotron signal with a linewidth of less than 1 Hz was observed this way, thus being our first *direct* cyclotron measurement of antiprotons with a linewidth resolution of less than 10^{-8}. We can also observe locked axial signals as a function of a weak cyclotron drive as a means of indirectly measuring the cyclotron resonance. This method may prove to be more sensitive than the direct cyclotron observations and has already been used by others to study a single proton in a much smaller trap [72].

As seen in Fig. 9.4(b) the sensitivity of the locked axial motion to cyclotron excitation is not yet significantly better than the direct cyclotron observations. As we saw in Chapter 6 with electrons, the sensitivity of the locked axial signal to the cyclotron excitation depends upon the achievable signal to noise to detect changes in the axial frequency $\Delta\nu_z$ and on the mechanism to couple energy in the cyclotron motion to the axial motion. Magnetic bottles and/or anharmonicity are effective in coupling the motions at some level, but both mechanisms introduce perturbations and possible systematic shifts on the measured eigenfrequencies. One way to avoid the need for such coupling mechanisms is to use phase sensitive detection techniques directly on the cyclotron motion though experimentally this is more difficult to implement than axial detection. Another technique is to apply rf voltages on the sideband drives at the sum or difference frequencies of the modes to be coupled. A short pulse can be used and if the duration and amplitude are correctly adjusted, such a pulse can exchange the motion between the two modes. An application of the technique at the magnetron sideband $\nu_c' + \nu_m$ has recently been applied to cool the magnetron motion of heavy ions [85]. Another recent

application using the axial sideband ν_c' - ν_z has been used to couple the cyclotron and axial motions for damping and detection of the cyclotron motion of single ions [21,22].

9.2.2 Cyclotron Motion

The direct detection method described detects the residual heat in the confined antiprotons. The method relies on the amplitude of the induced signal which depends on trap size, particle number and particle temperature. Ultimately there exist limitations to such a scheme, because large particle amplitudes and numbers can contribute to undesirable systematic effects. Therefore we continue to develop other more sensitive methods of direct particle detection to improve signal to noise, thus requiring fewer particles and smaller amplitudes.

One way to increase signal to noise is to observe the phase of the motion analogous to the schemes outlined with axial detection techniques. Eliminating direct feedthrough of the phase defining drives is more difficult since it can involve modulating the magnetic field. We have examined three different schemes to minimize feedthrough. At times, we have added a fraction of the drive signal to the detection line and adjusted the phase and amplitude to cancel the direct feedthrough. A factor of 50 in rms voltage reduction of the direct feedthrough signal is easily obtainable. Another way to realize such cancelation is to drive on opposite segments of the quad ring electrode in a balanced drive configuration [97]. By properly adjusting the phase of the signals to the two opposite segments, the direct feedthrough signal observed across the remaining segments is minimized.

For active drive techniques we can also minimize direct feedthrough by alternating the drive and detect cycles. To demonstrate this, we have adapted electronics developed for our pulsed NMR system to apply a strong drive pulse, and alternate it with the detection cycle. We show in Fig. 9.5 the detected cyclotron response signal mixed down to about 1 kHz. Different applied trapping voltages indicate that the visible ringing is from the trapped antiprotons.

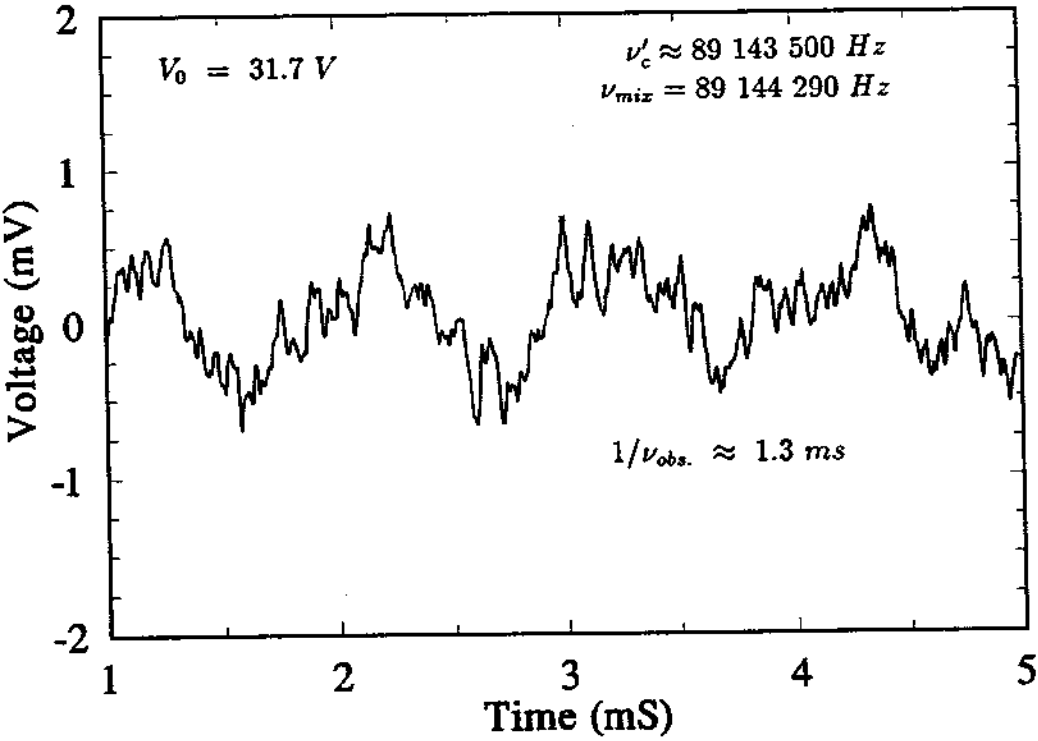

Figure 9.5: Oscillations in the directly detected ν_c' signal after strong pulsing.